LBNL-39008

PREPARATION AND PROPERTIES OF SPIN-COATED Nb_2O_5 FILMS BY THE SOL-GEL PROCESS FOR ELECTROCHROMIC APPLICATIONS

Nilgün Özer[1], Din-Guo Chen[2] and Carl M. Lampert[3].

[1] Istanbul University, Faculty of Science , Department of Physics, Vezneciler, Istanbul, Turkey
[2] YTC America Inc. 550 Via Alondra, Camarillo, CA 93012, USA
[3] University of California, Lawrence Berkeley National Laboratory, Building Technologies Program MS.62-203, 1 Cyclotron Road, Berkeley, CA 94720, USA

ABSTRACT

The preparation and properties of Nb_2O_5 coatings made by the sol-gel process were investigated. The films were deposited by spin coating on In_2O_3:Sn/glass and quartz substrates from a polymeric solutions of niobia derived from niobium ethoxide . The films were characterized by investigation of the stoichiometry, refractive index, optical transmission, electrochemical behavior, and the microstructure. X-ray diffraction (XRD) studies showed the films to be amorphous for heat treatments below 450 °C. X-ray photoelectron spectroscopy (XPS) measurement revealed the O:Nb atomic stoichiometry to be 5:2. Cyclic voltammetric (CV) measurements showed that the Nb_2O_5 / I M $LiClO_4$-propylene carbonate system exhibits electrochemical reversibility beyond 1200 cycles without change in performance. "In situ" UV-VIS-NIR spectroelectrochemical measurement revealed that Nb_2O_5 films exhibit an electrochromic effect in the spectral range $300<\lambda<2100$ nm and remain unchanged in the infrared spectral range. The change in visible transmittance was 40% for a 250 nm thick electrode. XPS spectra indicate that Nb(V) is reduced to a lower valence state Nb(IV) in colored state with injected Li^+. The bronze coloration is due to a simultaneous injection of electrons and Li^+ ions into Nb_2O_5. The sol-gel deposited Nb_2O_5 films are useful for cathodically coloring electrochromic electrodes in electrochromic devices.

1. INTRODUCTION

In recent years, transparent electrochromic devices received growing interest as energy efficient windows or switchable mirrors in cars (1). A large number of transition metal oxides such as WO_3, NiO_x, V_2O_5, MoO_3, TiO_2, MnO_2, Nb_2O_5 and Cr_2O_3 have been investigated as electrode materials for electrochromic devices (2-6). One of the promising electrochromic materials for use as a primary coloring electrode is NiO_x (1,7,8). There has been continued interest in finding a complementary electrode for NiO_x, cathodically coloring Nb_2O_5 is a possible candidate. Also, Nb_2O_5 can be used as a substitute for WO_3 (9). It may be possible to couple Nb_2O_5 with materials such as V_2O_5, IrO_2 and CoO, that have been used with WO_3 (10-12).

Nb_2O_5 films are readily fabricated by rf sputtering, magnetron sputtering (9,13), anodic oxidation (14), synthetic routes (15) and by the sol-gel process (16,17). In this study we investigated the structure, optical properties, and electrochemical behavior of Nb_2O_5 films deposited by sol-gel spin coating. In this study, we present characterization of sol-gel deposited Nb_2O_5 films. The major advantages of the sol-gel process are good chemical and mechanical stability, high porosity, potential for a homogeneous coating over a large-area and ease of microstructure control (18) . These factors can influence the kinetics, durability, coloring efficiency and charge capacity in electrochromic electrodes (19). Included in this study is the analysis of optical properties and switching properties using ellipsometry, voltammetry, spectroscopy, X-ray diffractometry and X-ray photoelectron spectroscopy.

2. EXPERIMENTAL PROCEDURE

2.1 Preparation of solution

The coating solutions were prepared by hydrolytic polycondensation. Niobium ethoxide ($Nb(OC_2H_5)_5$ 99.95 %, Aldrich Chem. Co. Milwaukee, WI) was used as molecular precursor. . The starting solution was prepared by first mixing one part niobium ethoxide (absorbed water of 3 % by weight), with 2/3 part ethanol and 0.003 part acetic acid (CH_3CH_2OH) by volume, while . stirring. The stirring of the solution was continued for 15 min. The solution was then diluted with ethanol to bring the $Nb(OC_2H_5)_5$ to C_2H_5OH ratio to 20. A clear light yellow solution was obtained after stirring for 2 hours. Addition of acetic acid played a specific role in the sol-gel processing of niobia it is not only a catalyst but it forms ligands with alkoxide. In the presence of acetic acid the gelation time for $Nb(OC_2H_5)_5$ increased from 96 h to 1248 h. This effect was also observed during the sol-gel processing of titania (20) The final volume ratio of $Nb(OC_2H_5)_5 : C_2H_5OH : CH_3OOH$ was 1:20:0.003.

These reactions can be described as follows:

hydrolysis: $Nb(OC_2H_5)_5 + 5\ H_2O \dashrightarrow Nb\ (OC_2H_5)_4(OH) + C_2H_5OH$

condensation: $Nb(OC_2H_5)_5 + Nb(OC_2H_5)_4(OH) \dashrightarrow Nb_2O(OC_2H_5)_8 + C_2H_5OH$

the complete hydrolysis reaction can theoretically leads to pure oxide state :

$$2\ Nb(OC_2H_5)_5 + 5\ H_2O \dashrightarrow Nb_2O_5 + 10\ C_2H_5OH$$

2.2. Preparation of Nb_2O_5 coatings

The Nb_2O_5 films were spin-coated from the solution described above. The solution was stable for at least two months at room temperature (55% relative humidity). Since clean surfaces is important for proper adhesion of the coating (21) , microscope slides and In_2O_3:Sn (ITO) coated glass substrates (10 Ω /cm^2, Donnelly Corp. Holland, MI) were ultrasonically cleaned in acetone, rinsed in deionized water, washed with isoproponol, and dried at room temperature. The coatings were deposited by spin coating on an Integrated Technologies P-6000 Spin Coater at the spin rate of 1500 rpm for 45 seconds. As many as 15 sequential layers were deposited to attain the desired thickness. The thickness increment per layer was approximately 124 nm for each deposition cycle. For this purpose it was necessary to have a stable solution over the application period. The films were fired in a furnace for 1hr. at 150 °C before each coating application. Heating of the coatings between applications were necessary, because of the very slow room temperature drying. . The dried coatings were transparent, light yellow in color, hard, durable, and stable. All coatings were X-ray amorphous up to a firing temperature of 450 °C, above which a slightly crystalline structure appeared. The crystallized coating corresponds to the orthorhombic structure of Nb_2O_5.

2.3. Characterization of the coating

Prior to the optical and structural investigations, the deposited films were exposed to the ambient atmosphere. Scanning electron microscopy, X-ray photoelectron spectroscopy, UV- VIS- NIR spectroscopy, ellipsometry, impedance spectroscopy and cyclic voltammetry measurements were made on each Nb_2O_5 film.

Scanning electron microscopy (SEM), JEOL model JSM 6400 was used to examine the surface morphology of the films. A thin silver film was deposited on the samples to avoid charging of the surface. The structure of Nb_2O_5 films was investigated by X-ray diffraction (XRD). The XRD study was carried out on a Siemens Kristalloflex X-ray diffractometer with a Ni-filtered Cu K_α excitation. X-ray beam was incident at 1 degree and the scan rate was 0.05 degree per step and 6 seconds per step for all measurements.

X-ray photoelectron spectroscopy (XPS). was used to identify chemical composition of the films. XPS spectrum was recorded on a Kratos XSAM 800-MCD spectrometer with Mg K_α X-ray source at 1253.6 eV. The background pressure of the system was approximately 5×10^{-9} torr. The spectrometer was calibrated for each experiment so that the Au ($4f_{1/2}$) electron binding energy was at 83.3±0.1 eV and adventitious carbon occurred at 285±0.1 eV.

The refractive indices of the coatings were determined by a Sopra model SE 4G spectroscopic ellipsometer over the 300-800 nm wavelength range. Three to five measurements were averaged for each data point. The dispersion curve was obtained by using Cauchy polynomial curve fitting. A Perkin-Elmer Lambda 9 double-beam spectrophotometer was used for spectral normal transmittance $T(\lambda)$ measurements.

The ionic conductivities of the Nb_2O_5 films were derived from a.c. complex impedance spectroscopy. The equipment used was a computer-controlled Schlumberger, SI 1260, Impedance gain analyzer. The analyzer was driven by a PAR model 273 potentiostat/galvanostat with an electrochemical interface. Data collection and analysis was done by computer. Cyclic voltametric measurements were performed with a PAR digital coulometer and a Hewlett-Packard X-Y recorder. The electrochemical cell consisted of a sealed three-electrode cell. Nb_2O_5 deposited on a ITO glass substrate was used as a working electrode. Lithium metal was used as the counter-electrode and reference electrodes. The electrolyte was anhydrous 1 M $LiClO_4$ in propylene carbonate (PC). Single or multi-scan cyclic measurements were performed within and at the potentials of 1.3 and 4.0 V versus Li.

The thickness of the films were measured by a Dektak II (Veeco Inst. Inc.) surface profiler having a maximum resolution of 0.5 nm/100 nm. Film thickness was 140 nm for a single layer coating deposited at a spinning rate of 1500 rpm.

3. RESULTS AND DISCUSSION

3.1 Formation and chemical analysis of as-deposited coatings.

To produce transparent and uniform Nb_2O_5 coatings the precursor solutions must be clear and not cloudy. First, we studied the variation of alkoxide content, catalyst type and solvent in the solutions to achieve this Next, we investigated the coatings deposited onto both glass and ITO coated glass substrates by the method discussed in subsection 2.1. The thickness of Nb_2O_5 coatings is a function of spinning rate (V_s). Lower spinning rates for solutions with the same viscosity produced thicker films. Film thicknesses between 83 and 178 nm were obtained by varying the spinning rate from 3000 to 1000 rpm.

A typical surface SEM view of a the Nb_2O_5 films is shown in Fig.1. It was found that the film surface was relatively smooth with few pinholes or microcracks over the size of the sample (5 cm^2). SEM cross-section micrographs show that Nb_2O_5 films are very uniform. The XRD patterns of a 210 nm thick Nb_2O_5 film on a glass substrate, as-prepared and after annealing, are shown in Fig. 2. The sol-gel deposited niobia films are typically amorphous. These films crystallize after heat treatments at or above 450 ^oC. Fig. 3 shows a wide-range XPS spectrum of niobium oxide film on a soda-lime glass substrate. The only impurities seen in the film are sodium (from the glass) and carbon. The stoichiometry of the films, given as ratio of oxygen to niobium (O:Nb) and was found to be 2.49. This ratio was computed from the area under the XPS peaks. We found for films deposited on different substrates the O:Nb ratio was within 2.49±0.02. All films showed binding energies for niobium and oxygen within normal experimental error (±0.2 eV). The measured binding energies are in agreement with standard Nb_2O_5 . The corresponding peak positions for niobium oxide films are listed in Table 1.

Table 1. Binding energies for Nb_2O_5 samples

parameter	film on glass d=120 nm	film on ITO d=122nm	rf magnetron sputtered (9)
Nb $3d_{5/2}$ (eV)	207.3	207.2	207.2
Nb $3d_{3/2}$ (eV)	210.1	210.1	210.0
$(3d_{3/2}-3d_{5/2})e$	2.8	2.9	2.8
O 1s (eV)	530.6	530.5	530.4
Ratio O: Nb	2.49	2.48	2.58

3.2. Optical Properties

The optical properties of Nb_2O_5 films were studied to determine the spectral n and k values, transmittance and uniformity. These values helped indicate the deposition-densification conditions to make the best films. The optical parameters (refractive index and optical band gap) for as-deposited films were determined by an ellipsometer and UV-VIS-NIR spectrophotometer in the $0.3 < \lambda < 2.5$ µm wavelength range.

Fig.4 shows transmittance spectra for a single layer and 3 layer niobia coating. These measurements are relative to a quartz substrate. The niobia absorption edge is noted at about $\lambda = 0.4$ µm. For the thicker film we see interference effects between the substrate and film. Fig. 5 shows the spectral dependence of the refractive index value, n of Nb_2O_5 films taken with an ellipsometer. As can be seen, the refractive index increases sharply for $\lambda < 0.4$ µm. The sharp increase in $n(\lambda)$ at shorter wavelengths is connected with band-to-band electronic transitions. The optical band gap, Eg=2.8 eV, was determined from the transmission data near the absorption edge (5). For the niobia films, the refractive index and extinction coefficient was n=1.82, and k= $3x10^{-4}$ at λ=0.53 µm. We observed an increase in refractive index and extinction coefficient values with increasing firing temperatures. Also, the Nb_2O_5 films were found to be nondispersive at $\lambda > 0.55$ µm. These values are lower in comparison to those for Nb_2O_5 films deposited by other techniques such as anodic oxidation, CVD, and reactive sputtering. The optical properties of Nb_2O_5 vary with the deposition technique. The refractive indices vary from n=2.1 to 2.4 with band gap values ranging from 3.2 to 3.9 eV for Nb_2O_5 films made by evaporation, sputtering, anodization and CVD (22).

3.3 Electrochemistry and Impedance Spectroscopy

Cyclic voltammetry (CV) was performed on Nb_2O_5/ITO/glass electrodes in an electrolyte of 1 M $LiClO_4$ in propylene carbonate (PC) at room temperature. Fig. 6 shows the cyclic voltammogram of Nb_2O_5 films for a range of sweep rates for as-deposited films. These results are similar to that of previously reported dip-coated sol-gel Nb_2O_5 (23). The curve shows a single oxidation-reduction cycle. At about 1.5 V (vs. Li) we see the anodic current peak. The cathodic and anodic charge capacity is approximately equal at $2x10^{-2}$ C/cm^2, for a sweep rate of 20 mV/s. We note that the present data are comparable with those in ref.23. The Nb_20_5 film colored to bronze at low positive potentials, eg. 1.7 V (vs. Li) . This coloration is the result of Li^+ and e^- insertion into the film. The film bleaches by application of an anodic potential which results in Li^+ and e^- extraction. The coloration process began around 2.1 V (vs. Li) and deepened at lower voltages. The color started to bleached at around 1.5 V (vs. Li). Long term cycling (several days) at room temperature show that Nb_20_5 films were quite stable. We see no significant change (no more than 1 mC/cm^2) in the spectra compared to the as-deposited film. This shows that the electrochemical Li^+ insertion/extraction is reversible. The voltammetry indicate that Nb^{5+} is reduced to a lower valence state Nb^{4+} by lithiation, which is recovered to the original valency through delithiation.

Impedance spectroscopy was used to determine ionic conductivity of Li^+ in niobia films. Fig 7 shows a complex impedance plane diagram, which consists of a semicircle. at the high frequency region and a straight line with a slope of 40° in the low frequency region. This behavior is typically seen in measurements of lithium conductors using blocking electrodes (23). The complex impedance data can be analyzed in terms of an equivalent circuit model. The equivalent circuit for this system is shown in the inset in Fig. 7. This circuit is valid for the diffusion of ions into an oxide electrode under an applied electric field. In Fig 7, R_e is the uncompensated ohmic resistance of electrolyte and electrode, C_d is the double layer capacitance of the electrode-electrolyte interface, R_i is the charge transfer resistance at the substrate/Nb_2O_5 interface, C_g is the geometric capacitance between the electrodes. The lithium conductivity was determined from the bulk resistance (the diameter of the semicircle) and the geometrical factors (shape, thickness and electrode area)(24). It was found that Li^+ conductivity was between 4.4×10^{-9} and 5.6×10^{-8} S/cm^2 for different films. The thicker films ($d<0.3$ μm) gave the highest lithium conductivity.

The UV/VIS/NIR transmittance spectra of Nb_2O_5/ITO/glass electrode in the reduced and oxidized states are shown in Fig.8. The Nb_2O_5 film is bronze under the applied potential of 1.3 V (vs Li). The electrode was colored at 1.8 V (vs. Li) A decrease in transmittance between 0.35 μm and 0.80 μm occurs under this applied potential. Using the weighted ordinate method, the photopic response for the colored and bleached states was found to be $T_p=0.46$ and $T_p=0.79$ respectively. A deeper coloration ($T_p=0.32$) can be obtained at 1.3 V (vs. Li). The film became transparent again when the bleaching potential of 3.6-3.8 V (vs Li) was applied for a few seconds (15 s).

3.3 Chemical analysis of cycled films

The XPS binding energy curves for niobia films cycled 1200 times are shown in Figs. 9,10. Curves are shown for the reduced and oxidized states. In Fig. 9 are the curves for Nb (3d) and in Fig 10 are the O(1s) spectra. The corresponding peak positions for these films are summarized in Table 2. For as-deposited films, a pair of peaks due to Nb $3d_{3/2}$ and $3d_{5/2}$ core levels are observed at the binding energies of 210.1±0.1 and 207.3±0.1 eV respectively. These values correspond to Nb_2O_5 (25). After coloration, the peaks due to Nb $3d_{3/2}$ and $3d_{5/2}$ are observed at 209.8±0.1 and 207.0±0.1 eV. These values are lower by 0.3 eV than that observed in as-prepared films. After bleaching, the Nb (3d) peaks are again observed at 210.1±0.1 eV and 207.3±0.1 eV. This shift has been observed in battery electrodes during chargedischarge reactions and corresponds to the colored and bleached conditions of the electrode (26).

The corresponding O 1s spectra of Nb_2O_5 is shown in Fig. 10. The spectrum exhibits a single peak centered at 530.6±0.1 that can be assigned to O^{2-}. The binding energy of 530.5±0.1 eV fits well with data in the literature, and corresponds to the O^{2-} anion in niobium oxides (27). The O 1s peak is shifted to a higher binding energy of 532.5±0.1 eV after lithiation and charging. After delithiation, the O 1s peak is observed at 530.5±0.1 eV, the same value before lithiation.

From the Li 1s spectra of the bleached films (Fig 11), it is found that the Li 1s peak is located at 53.9±0.1 eV. After lithiation, the peak shifts to a higher binding energy by about 0.6 eV. The Li 1s peak is located at about 54.5±0.1 eV. The Nb:0 atomic ratio of the oxide was 0.40 for the uncycled film. After 1200 cycles this ratio remains the same. The XPS spectra for the uncycled film was identical to the bleached film after 1200 cycles. Also, the spectra of colored film remained the same over 1200 cycles.

Table 2. Binding energies for colored and bleached niobium oxide showing both uncycled and cycled films

parameter	as-prepared d=195nm	colored 1 cycle	colored 1200 cycle	bleached
Nb $3d_{5/2}$(eV)	207.3	207.1	207.0	207.3
Nb $3d_{3/2}$(eV)	210.1	209.9	209.9	210.2
Δ 3d (eV)	2.8	2.8	2.9	2.9
O 1s (eV)	530.6	532.5	532.4	530.5
Li 1s (eV)	-	54.4	54.5	53.9

4. CONCLUSION

Amorphous and transparent electrochromic Nb_2O_5 films were prepared successfully by a sol-gel spinning technique. The best film uniformity was observed at the spinning rate of 1500 rpm. Lithiation and delithiation process in this films in IM $LiClO_4$ - PC solution resulted in desirable changes (ΔT_{vis} 40 %) in optical transmittance. XPS examination showed the film consisted of $Li_xNb_2O_5$ in the colored state. Electrochemical cycling experiments have shown that the niobia film was stable for at least 1200 cycles with no change in performance. Nb_2O_5 is transparent, and the reduced form is brown.

Electrochemical measurements combined with XPS examination confirms that the reduction and oxidation reactions with lithiation (coloration) delithiation (bleaching) can be represented by:

$$\underset{\text{bleached}}{Nb_2O_5 + xLi^+ + xe^-} <-> \underset{\text{colored}}{Li_xNb_2O_5}$$

During lithiation Li^+ ions are incorporated into the oxide and at the same time Nb^{5+} is reduced to Nb^{4+} by accepting an electron. This process forms a colored intercalation compound, $Li_xNb_2O_5$. The reverse process reforms the clear state of Nb_2O_5. The high reversibility, stability and optical properties of lithium insertion make Nb_2O_5 thin films useful for transparent electrochromic devices as a counter electrode, particularly in nickel oxide devices

ACKNOWLEDGMENTS

This work was supported by the Assistant Secretary for Energy Efficiency and Renewable Energy, Office of Building Technologies, Building Systems and Materials Division of the U.S. Department of Energy under Contract No. DE-AC03-76SF00098.
The authors wish to thank Dr. Temel Buyuklmanli, Material Characterization Laboratory, Pennsylvania State University, for performing XPS measurements.

REFERENCES

(1) C.M. Lampert and C.G. Granqvist, eds., Large-area Chromogenics: Material and Devices for Transmittance Control, SPIE Optical Engineering Press, Bellingham, WA,1990.

(2) C.G. Granqvist, Solid State Ionics 53-56 (1992) 479.

(3) C.M. Lampert, Thin Solid films, 236 (1993) 6.

(4) N.Özer- D.G.Chen and J.H. Simmons, Ceram. Trans.20(1991) 253.

(5) M.Nabavi, S.Doeuff, C. Sanchez and J.Livage, Mater.Sci.Eng. B3(1989) 203.

(6) A.Donnadieu, Mater.Sci.Eng.,B3(1989) 185.

(7) S.Yamada, T.Yoshioka, M.Miyashita, K.Urabe and M.Kitao J.Appl. Phys. 63-6 (1988) 2116.

(8) S.Passerini and B.Scrosatti, Solid State Ionics 53 (1992) 520.

(9) M. Rubin, X.Yao and C.M. Lampert, Proc. of 1st Inter. Meet. on Electrochromism, Venice, Italy, Oct.19-21,1994, to be pub.

(10) P. C.Yu, T. E. Haas, R. B. Goldner and S. F. Cogan, Material Research Society Symposium Proceeding, 210(1991) 63.

(11) D.R.Rauh and S.F.Cogan, Solid State Ionics, 28-30 (1988) 1707.

(12) R.J.Colton, A.M. Guzman and J.W.Rabalais, J.Appl. Phys., 49 (1978) 409.

(13) P.C.Yu, T.E.HAss and R.B.Goldner, Electrochemical Society Symposium Proceedings 94-2(1993) 122.

(14) M.A.B.Gomes, L.O.S.Bulhoes, S.C.Castro and A.J.Damio, J.Electrochem.Soc. 137(1990)3067.

(15) R.C. Faria and L.O.S. Bulhoes, J.Electrochem. Soc. 141(1994)L29.

(16) P.Griesmar, G.Papin, C.Sanchez and J.Livage, Chem.Mater., 3(1991)335.

(17) B.Ohtani, K.Iwai, S.Nishimoto, and T.Inui, J.Electrochem.Soc. 141(1994)2439

(18) C.J.Brinker and G.W.Scherer Sol-Gel Science, Academic Press, San Diego, CA(1990)

(19) K.Machida and M.Enyo, J.Electrochem. Soc. 137(1990)1169.

(20) C. Sanchez, J. Livage, M. Henry, F. Baboneau, J. Non-Cryst. Solid, 100 (1988) 65

(21) D.M.Mattox, Thin Solid Films 53(1978)81.

(22) C.G.Granqvist,Electrochromic Metal Oxides, Elsevier,Amsterdam (1995) in press.

(23) P.Griesmar, G.Papin, C.Sanchez and J.Livage, Chem.Mater., 3(1991)335.

(24) C.Bohnke and O.Bohnke, Solid State Ionics, 39(1990)195.

(25) V.E. Henrich, P.A. Cox, The Surface Science of Metal Oxides Cambridge University Press, Cambridge, 1994.

(26) N.Kumagai, K.Tanno, T.Nakajima and N.Watanabe, Electrochimica Acta.,28(1983)17.

(27) P.H.Holloway and G.C.Nelson, J.Vac. Sci. Technol. 16(1979)793

Figure Captions

Fig 1. Plan view of SEM micrograph of sol-gel deposited Nb_2O_5 film (210 nm thick) deposited on soda-lime glass.

Fig 2. XRD patterns of Nb_2O_5 films:(a) as-prepared. (b) fired at 500 °C on soda-lime glass substrate.

Fig 3. XPS survey scan of Nb_2O_5 films.

Fig 4. Spectral normal transmittance for a single layer (140 nm thick) and multilayer (340 nm thick) Nb_2O_5 coatings.

Fig 5. Wavelength dependence of refractive index of Nb_2O_5 films.

Fig 6. Cyclic voltammograms for a 210 nm thick Nb_2O_5 film on ITO coated glass electrode in IM $LiClO_4$ - PC solution. Data are given for different voltages and sweep rates.

Fig 7. Typical complex impedance diagram of an amorphous sol-gel Nb_20_5 (230 nm thick) coating. The inset shows the equivalent circuit used for analysis (electrode area = 6.25 cm^2).

Fig 8. Transmittance spectra of Nb_2O_5 films on ITO coated glass electrodes: oxidized (bleached) at 4.0 V and reduced (colored) at 1.3 V (vs Li).

Fig 9. XPS spectra of Nb_2O_5 film in the Nb(3d) region at colored and bleached states.

Fig 10. Typical 0(1s) spectra of colored and bleached Nb_2O_5 film.

Fig 11. Li(1s) XPS spectra of a colored and bleached Nb_2O_5 electrode.

Fig 1

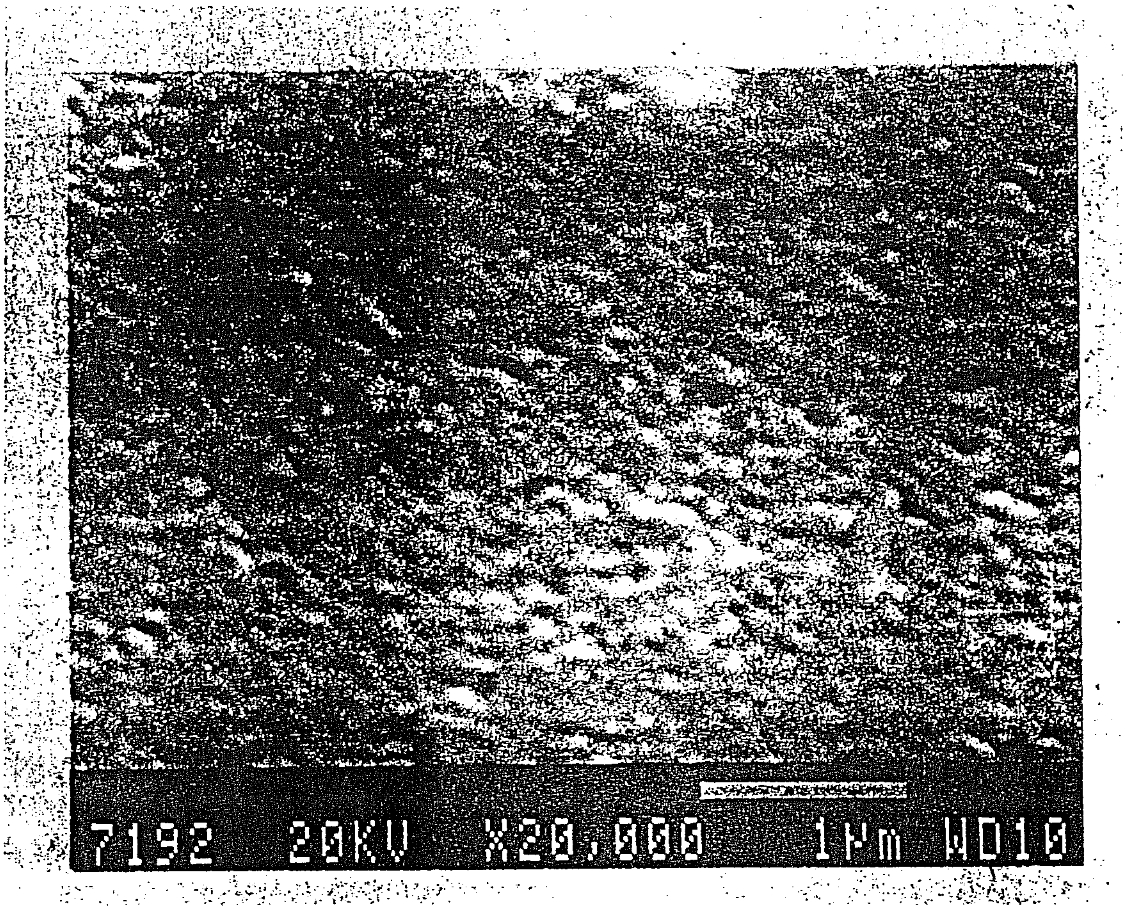
7192 20KV X20,000 1μm WD10

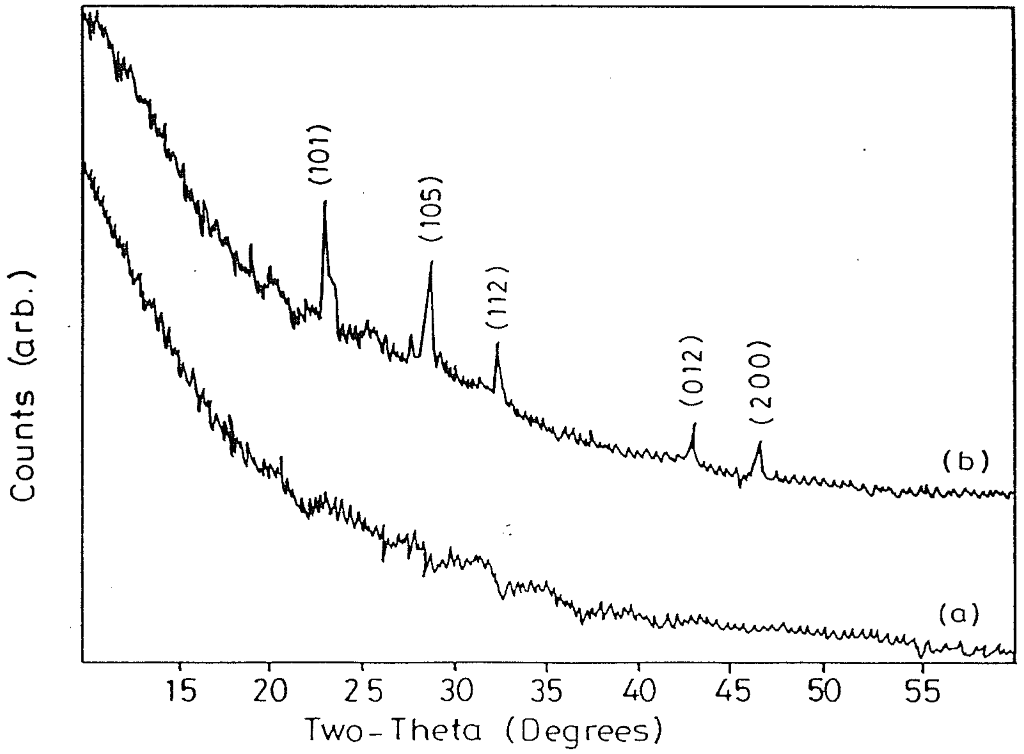
(101)
(105)
(112)
(012)
(200)
(b)
(a)
Counts (arb.)
15
20
25
30
35
40
45
50
55
Two-Theta (Degrees)

Fig. 2

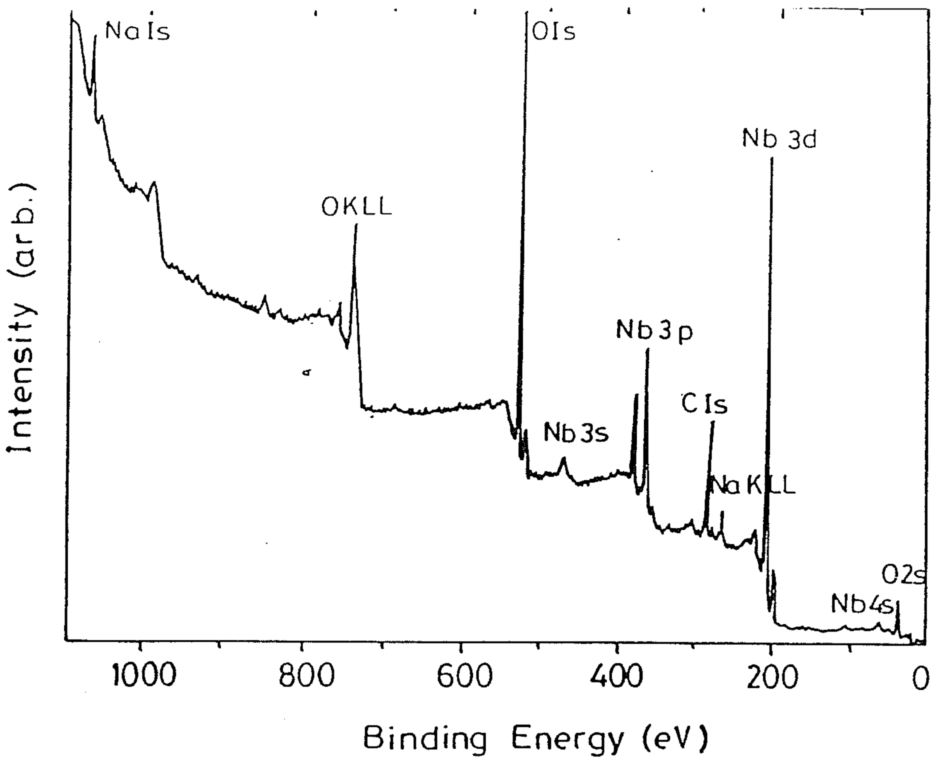
Intensity (arb.)
NaIs
OKLL
OIs
Nb 3d
Nb3p
Nb3s
CIs
NaKLL
O2s
Nb4s
1000
800
600
400
200
0
Binding Energy (eV)

Fig. 3

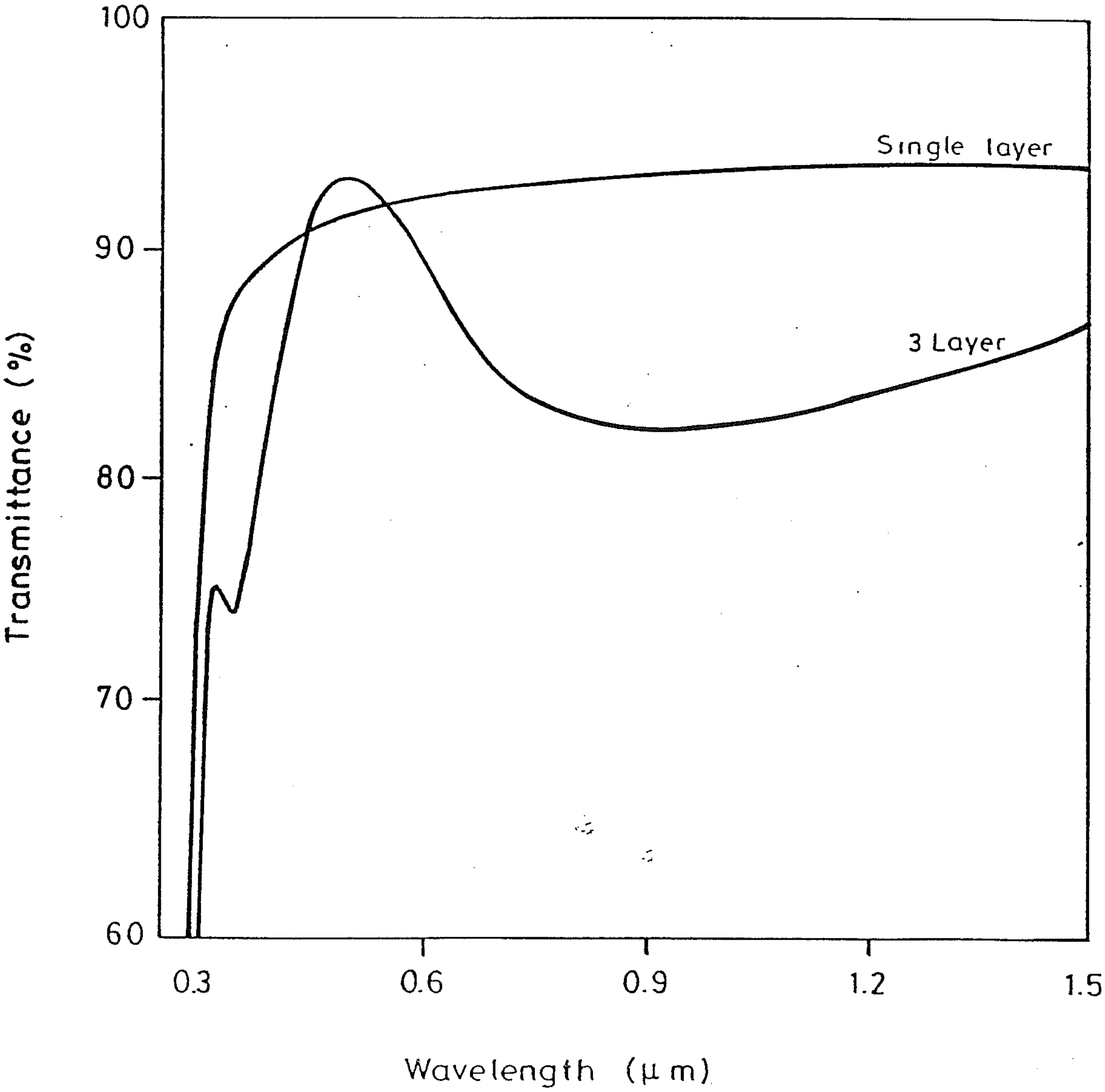
100
90
80
70
60
Transmittance (%)
Single layer
3 Layer
0.3
0.6
0.9
1.2
1.5
Wavelength (μm)

Fig. 4

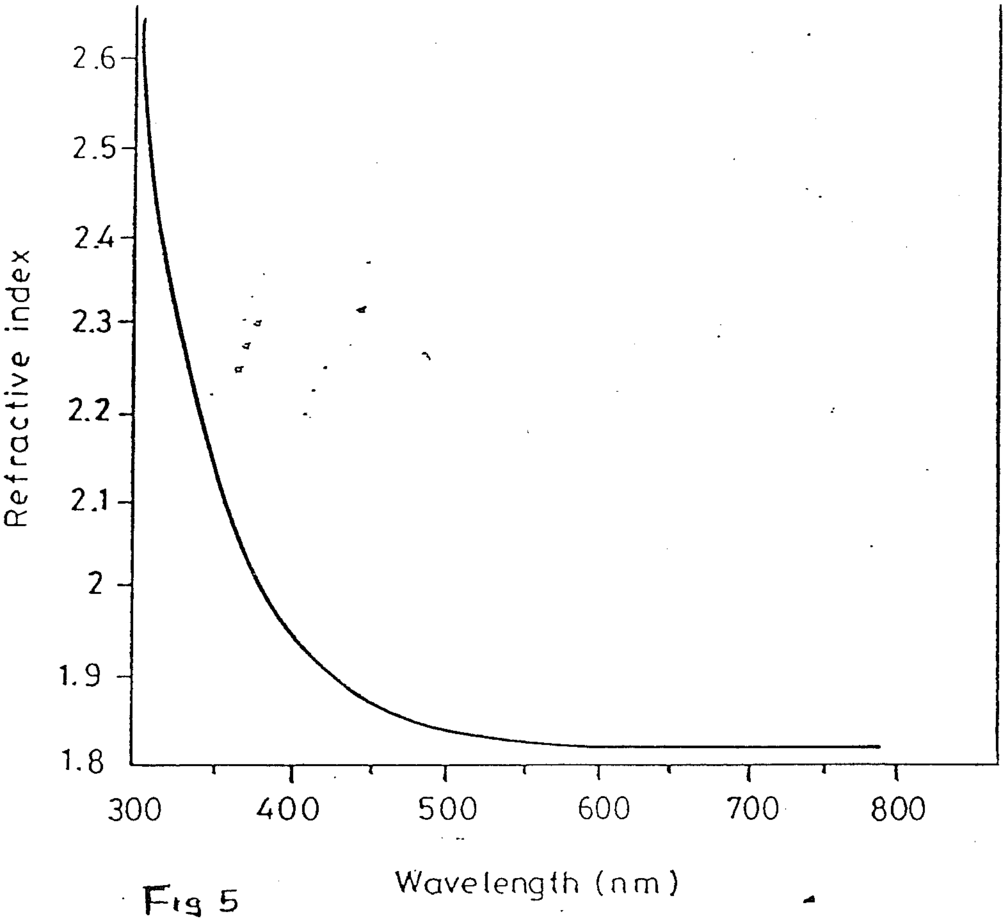

Refractive index
2.6
2.5
2.4
2.3
2.2
2.1
2
1.9
1.8
300
400
500
600
700
800
Wavelength (nm)

Fig 5

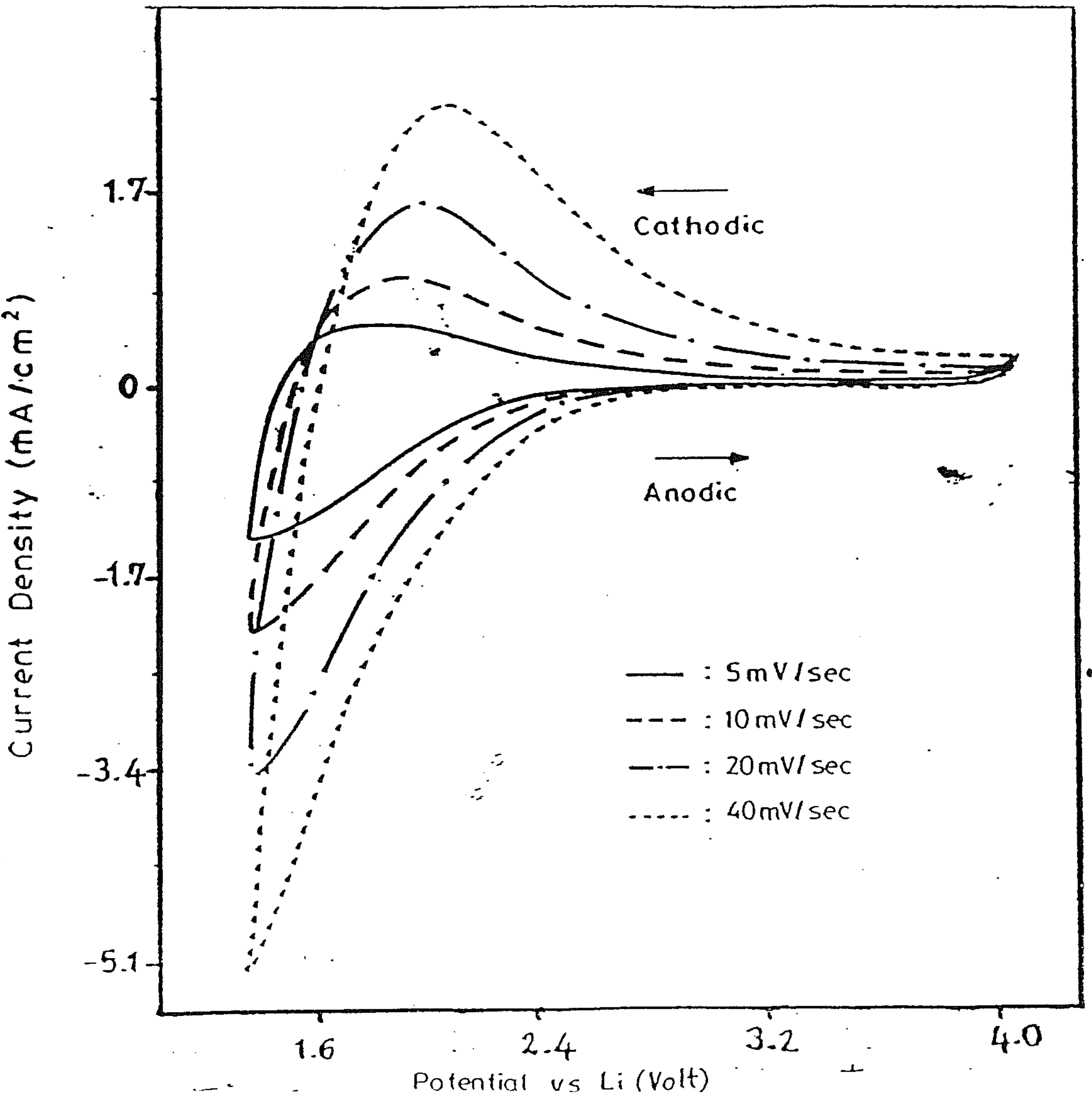

Current Density (mA/cm²)
1.7
0
-1.7
-3.4
-5.1
Cathodic
Anodic
: 5mV/sec
: 10mV/sec
: 20mV/sec
: 40mV/sec
1.6
2.4
3.2
4.0
Potential vs Li (Volt)

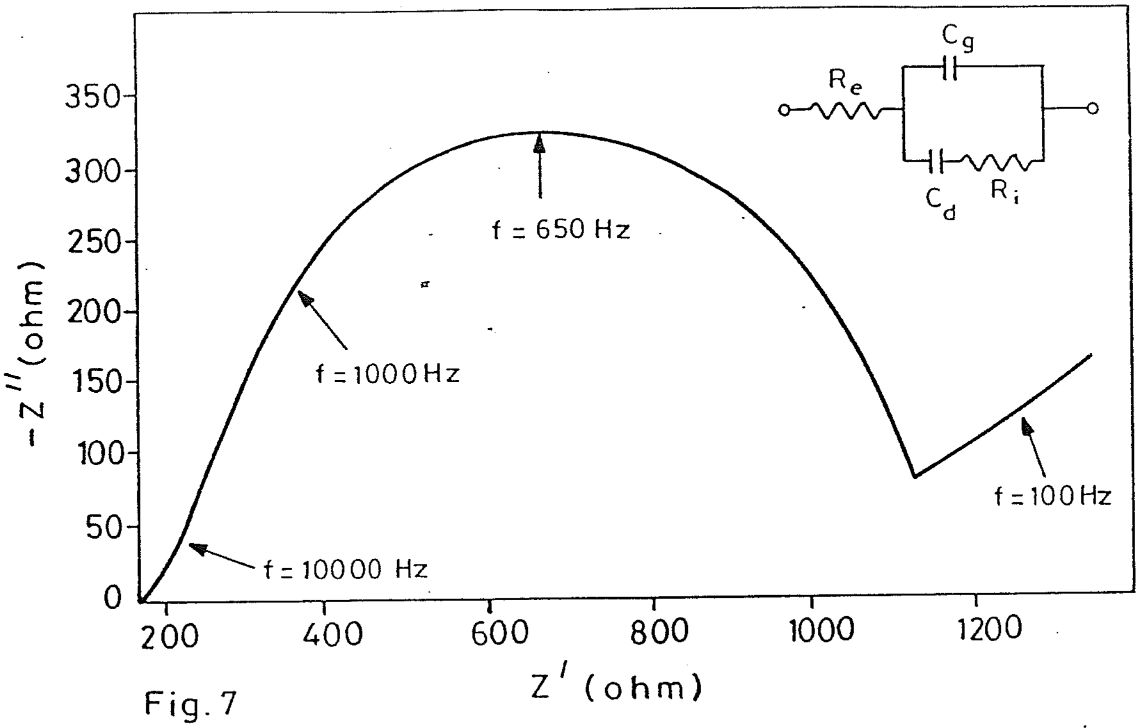

350
300
250
200
150
100
50
0
$-Z''$ (ohm)
200
400
600
800
1000
1200
Z' (ohm)
f = 650 Hz
f = 1000 Hz
f = 10000 Hz
f = 100 Hz
R_e
C_g
C_d
R_i

Fig. 7

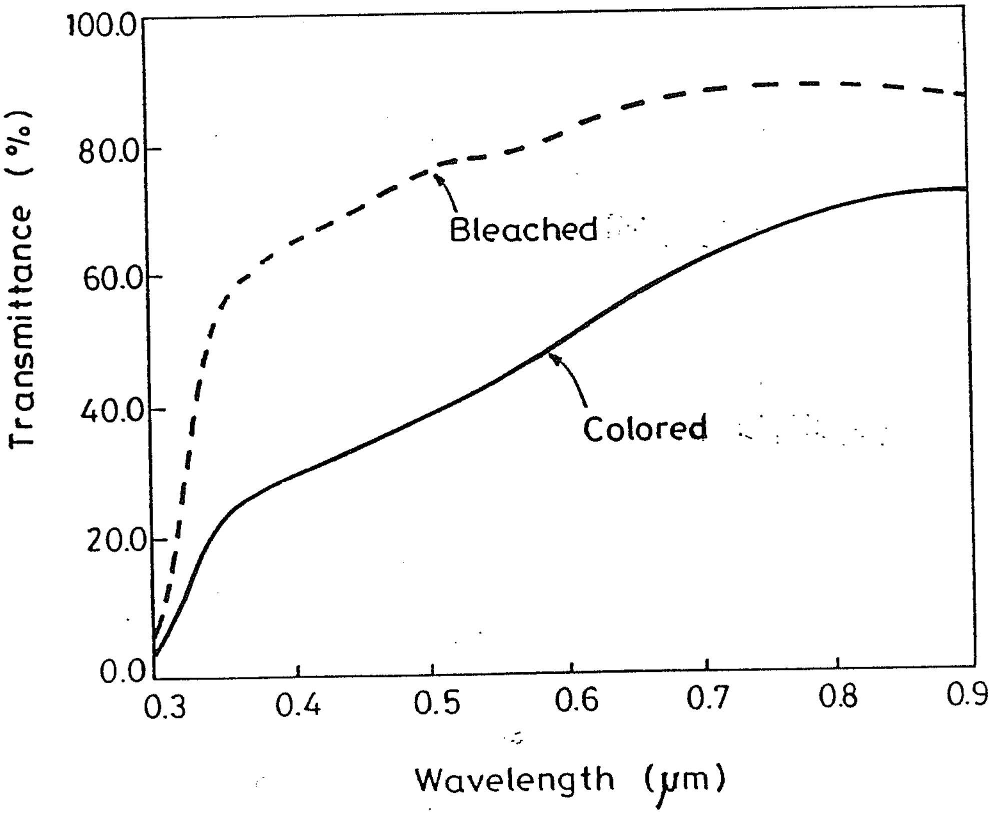

100.0
80.0
60.0
40.0
20.0
0.0
Transmittance (%)
0.3
0.4
0.5
0.6
0.7
0.8
0.9
Wavelength (μm)
Bleached
Colored

Fig. 8

Fig. 9

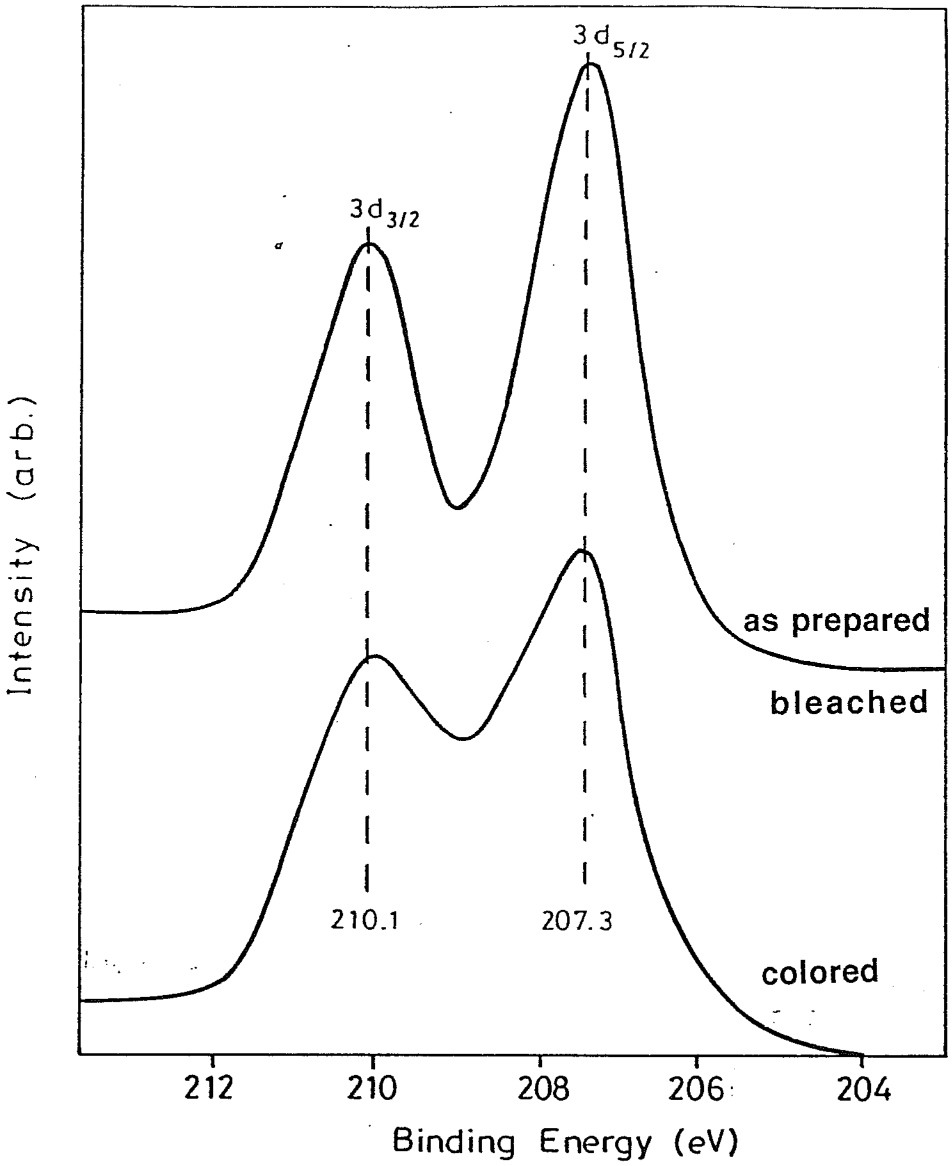
3d$_{5/2}$
3d$_{3/2}$
Intensity (arb.)
as prepared
bleached
colored
210.1
207.3
212
210
208
206
204
Binding Energy (eV)

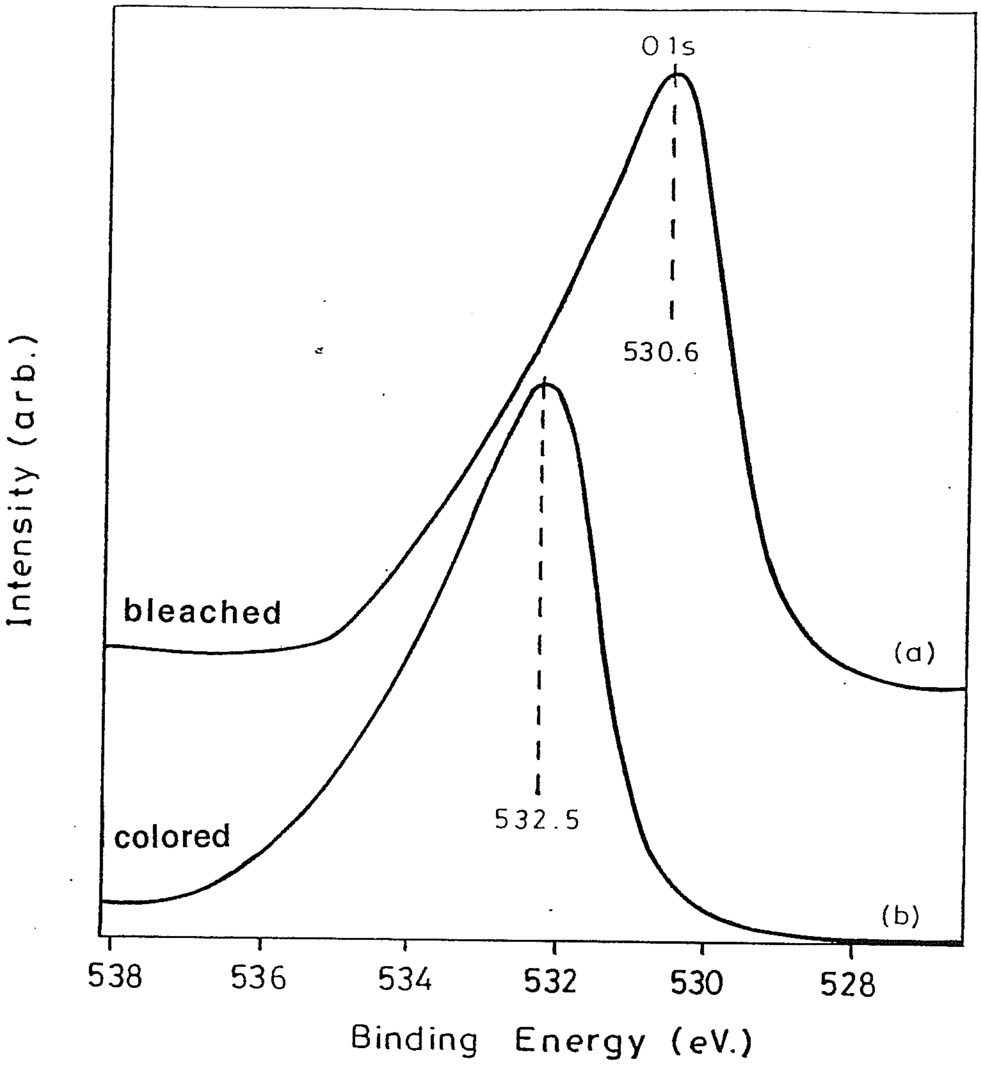
O1s
530.6
532.5
bleached
colored
(a)
(b)
Intensity (arb.)
538
536
534
532
530
528
Binding Energy (eV.)

Fig.10

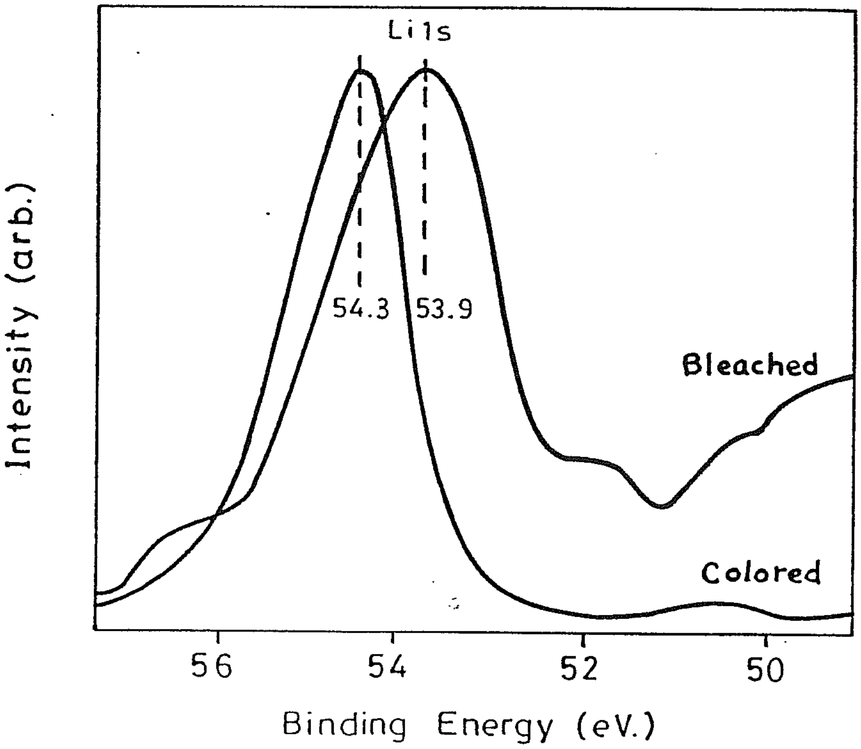
Li1s
54.3
53.9
Bleached
Colored
Intensity (arb.)
56
54
52
50
Binding Energy (eV.)

Fig.11